applied optics

Mapping distortion correction in freeform mirror testing by computer-generated hologram

Xuefeng Zeng,[1,*] Xuejun Zhang,[1] Donglin Xue,[1] Zhiyu Zhang,[1] and Jian Jiao[2]

[1]Key Laboratory of Optical System Advanced Manufacturing Technology (KLOMT), Changchun Institute of Optics, Fine Mechanics and Physics, Chinese Academy of Sciences, Changchun, 130033 Jilin, China
[2]Harbin University of Commerce, Harbin 150028, China
*Corresponding author: zengxf@ciomp.ac.cn

Received 3 July 2018; revised 15 October 2018; accepted 29 October 2018; posted 30 October 2018 (Doc. ID 337683); published 27 November 2018

Distortion can be introduced in null testing using computer-generated holograms for off-axis aspheres or freeforms with significant deviation. It leads to the failure of testing results to guide deterministic optical processing. In this paper, based on ray tracing and calibration marks applied to a mirror surface, a high-accuracy method is proposed to correct the distortion. The correction error is less than 1 mm. Second and fourth mirrors of a reflective telescope prototype with an F number of 6.5 and field of view of 76° are polished. In the process, distortion is corrected, and the position misalignment error is as small as 0.783 mm. For the sake of alignment, the two mirrors are fixed on a 790 mm × 390 mm SiC substrate. The root-mean-square value of the mirror surface error is 0.0433λ ($\lambda = 0.6328$ μm) after ion beam finishing.

https://doi.org/10.1364/AO.57.000F56

1. INTRODUCTION

Freeform surfaces described by a φ-polynomial or Zernike polynomial provide more design freedom to imaging systems without introducing new types of aberration; therefore, better performance can be expected [1–3]. However, high-precision testing of freedom surfaces is a challenging task [4].

With the development of optical testing and microelectronics technology, the computer-generated hologram (CGH) has been more and more widely used in optical testing [5]. CGH has testing accuracy superior to $\lambda/100$ [6,7]. It also has the advantages of small volume, light weight, and more design freedom. Compared with a traditional compensator, CGH is easily mounted, adjusted, and reused, and is indispensable to test freeform surfaces [8].

However, CGH also has some disadvantages, such as low diffraction efficiency and distortion. The former was extensively discussed and could be improved by using phase-type CGH, but the latter was seldom reported [3]. In CGH (both amplitude-type CGH and phase-type CGH), null composition testing for freeform or off-axis asphere, two-dimensional mapping distortion without rotational symmetry, was introduced in testing of the freeform by CGH. Since the caustic of the second fourth mirror (SFM) mirror reported in the following sections is big and the CGH fabrication limit is 180 mm, large mapping distortion exists in the test data. Such distortion will cause the polishing process to non-converge and must be corrected.

At present, there are two kinds of correction distortion methods for testing aspheric surfaces with null compensation in the published literature. The first correction method is used for coaxial aspheric surfaces with null lens compensation testing. In this method, it is considered that the mapping distortion is rotationally symmetrical along the radial direction of the aspheric parent mirror, so one-dimensional distortion fitting can be carried out based on the mirror fiducial, and the mapping distortion can be corrected. Because few fiducial points can be set on the mirror, the fitting accuracy of this method is low, and only one-dimensional fitting can be done; it cannot correct the projection distortion in freeform surface interference detection. Please refer to the literature [8]. Another correction method for projection distortion was proposed by Novak *et al.* of the University of Arizona. They used the method of covering regular meshes on the mirror surface to correct projection distortion. This method is similar to the previous method. Although two-dimensional fitting is realized with the help of grid plates, it is still difficult to increase the number of sampling points. Although the scope of application is extended, the correction accuracy of this method has not been effectively improved. The engineering application of this method is relatively complex, and the specific algorithm and accuracy are not given in the article. Refer to the following literature. Neither of these methods can meet the accuracy requirements of deterministic fabrication, such as the ion beam figure (IBF) [9].

In this paper, in order to realize high-accuracy distortion correction, a new method is presented based on the affine transformation of a testing light path. The method is presented based on the fact that the major resources of mapping distortion stem from the optical path between CGH and mirror, and

this part is high order, the denser the tracking points, the higher the accuracy. Therefore, the testing was separated into three parts. First, the nonlinear transform is done between coordinate systems of CGH and mirror by ray tracing. We can set the destiny of point on mirror very close together, so that, it is better to simulate the distortion than traditional methods the above mentioned. Second, the transmission sphere with an F number of 0.75 for a Fizeau interferometer will introduce cosine form distortion, and this distortion was calibrated. Third, the linear transform was done between the coordinate systems of CCD and CGH by many fewer fiducial points, which were pasted on the mirror under test (MUT). Their positions could be tested accurately. Owing to the high-accuracy measurement of marker position on the mirror, centroid algorithm and ray tracing method, the high accuracy of distortion correction could be achieved. The distortion correction theory of the proposed method will be presented in detail in Section 2. Experimental results will be shown in Section 3.

2. DISTORTION CORRECTION

A. Mapping from CGH to Mirror

The relationship between the mirror surfaces to the CGH can be obtained by ray tracing. As shown in Figs. 1(a) and 2(a), a concave even aspherical reflector whose radius is 2483 mm and the conic coefficient K is −2.1536 was tested with CGH. In order to show the relationship between distortion and the CGH position, two ordinary testing layouts were given. In these two examples, CGH was located at 2280 mm and 1596 mm away from the MUT. Uniformed grid rays were ejected along the mirror normal direction [Figs. 1(b) and 2(b)]. The intersection points at the distortion reference surface (e.g., considering the distortion at CGH and the reference surface on CGH) are shown in Figs. 1(c) and 2(c).

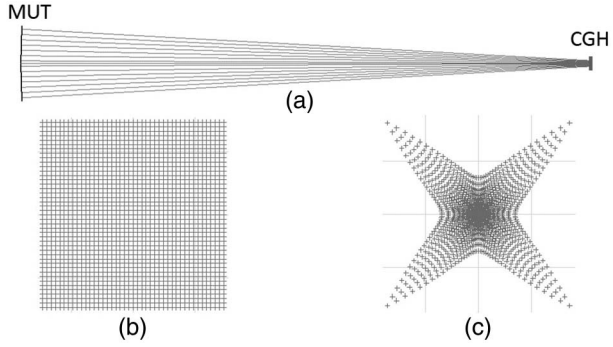

Fig. 1. Distortion of testing a concave even aspherical mirror with CGH: (a) testing layout, (b) uniform grid on the mirror under test, and (c) uniform grid mapping to the CGH.

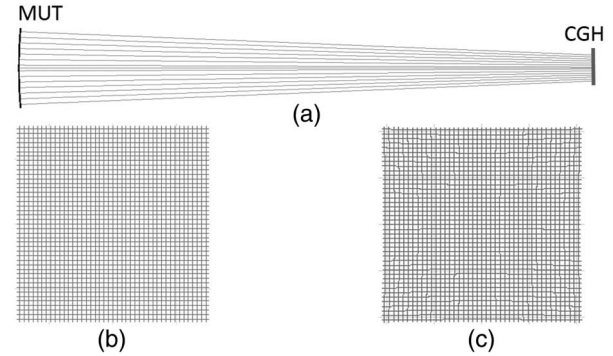

Fig. 2. CGH set at 1596 mm behind the mirror under test; distortion of testing a concave even aspherical mirror with CGH: (a) testing layout, (b) uniform grid on the mirror under test, and (c) uniform grid mapping to CGH.

From these two examples, we can find that the closer to MUT, the smaller the distortion, but the larger the CGH. So that CGH should choice a better location [10].

In order to describe the severity of the distortion, the calculation of mapping distortion for compensation interference testing needs to be defined. For the imaging system, the distortion is the difference between the ideal image height and the actual image height that intersects the main ray with the ideal image surface, which is different from imaging distortion. Mapping distortion in interference testing is actually due to the surface curvature, and caused by the nonlinear relationship between rays projected on mirrors with different curvatures. Due to the high-precision positioning requirements for optical processing, a new definition for distortion is given as follows. The geometric center of the mirror was set as the original point of the mirror, and the corresponding point on the reference surface was set as the original point of the distorted data. Then, distorted data were stretched linearly to the maximum circle radius, which covers the tested mirror (show as Fig. 3). The mapping distortion coefficient (K_D) was defined as the ratio of maximum deviation of the position to the actual position after expansion. K_D could be positive or negative, and the greater absolute value of K_D brings out more serious distortion.

Its equation is expressed as

$$K_D = \frac{R_i - (R_{ci} * R/R_c)}{R_i}. \tag{1}$$

For the examples in the graphs (Figs. 1 and 2), the distortion coefficient of the CGH reference surface at the distance of 2280 mm from aspherical surface is 0.599, and the distortion coefficient is 0.011 when it moves to 1596 mm, which is in full agreement with the actual situation, indicating that the definition of the coefficient satisfies the requirement of the CGH. In fact, the mapping distortion can be reduced by larger-sized CGH, but as the size of the CGH is limited, CGH design should be considered in accordance with the needs of the testing. As shown in Figs. 1 and 2, in different distances from

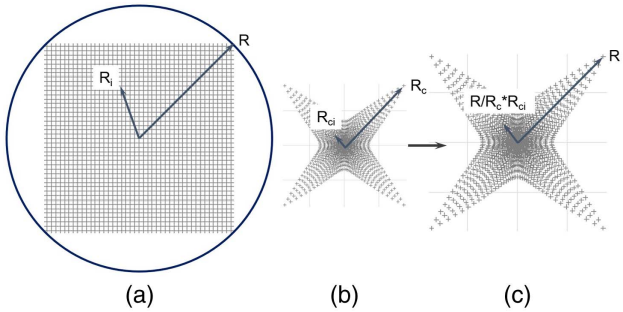

Fig. 3. Distorted data expansion linearly to uniform grid on reflector.

MUT, the distortion is different. On one hand, the closer to the caustic surface, the larger the distortion; on the other hand, the carrier frequency also has a slight effect on distortion. These factors need to be carefully balanced. CGH design and distortion balance work can be referred to in documents [7,10–22].

B. Distortion of ZYGO F0.75 Transmission Sphere

Through experiments, the cosine distortion relation was found in the F0.75 transmission of the Fizeau interferometer [10,23]. After simulation, the distortion form is shown in Figs. 4 and 5.

Because the internal structure of the interferometer is unknown, the distortion of the transmission sphere was obtained by experimental measurement. As shown in the measurement optical path (Fig. 6), a spherical surface with known points and R number of 0.8 was tested by the interferometer. The coordinates of the interference detection results were compared to the known points. As a result, the edge distortion coefficient of the F0.75 transmission sphere was 0.965 at the edge. In the actual testing, distortion was compensated according to the used position of the transmission sphere.

C. Mapping from CCD to Surface after Transmission Sphere

The mapping from mirror to CGH was established by ray tracing, and the mapping relation from CCD plane to VP plane (virtual plane after transmission sphere) was obtained based on affine transformation. As shown in Fig. 7, the mark coordinates (named P_{CCD}) and the coordinates on the VP (named P_{VP}) can be used to solve the affine transformation parameters. Other test data would be equivalently transformed based on the affine transformation parameters.

As shown in Fig. 7, in order to make the affine transformation parameters as constant, i.e., k and $\Delta\theta$, a new transformation coordinate system $x_a o_a y_a$ is needed. A pair of points on CCD and VP, i.e., P_{CCD0} and P_{VP0}, are shifted parallel to the origin of $x_a o_a y_a$, and other points are shifted by the same amount. The relationship between $(x_{\mathrm{VP}a}, y_{\mathrm{VP}a})$ and $(x_{\mathrm{CCD}a}, y_{\mathrm{CCD}a})$ can be expressed in the polar coordinate system as follows:

$$\begin{cases} r_{\mathrm{VP}a} = k r_{\mathrm{CCD}a} \\ \theta_{\mathrm{VP}a} = \theta_{\mathrm{CCD}a} + \Delta\theta \end{cases}, \tag{2}$$

where

$$\begin{cases} x_a = r\cos\theta_a \\ y_a = r\sin\theta_a \end{cases},$$

k is the zoom ratio, and $\Delta\theta$ is the rotation angle.

Hence, the affine transformation function can be expressed as the following equation set. The $(x_{\mathrm{CCD}}, y_{\mathrm{CCD}})$ was obtained from interference testing:

$$\begin{cases} x_{\mathrm{VP}} = k\sqrt{(x_{\mathrm{CCD}} - x_{\mathrm{CCD}o})^2 + (x_{\mathrm{CCD}} - x_{\mathrm{CCD}o})^2}\cos(\theta_{\mathrm{CCD}a} + \Delta\theta) + x_{\mathrm{CGH}o}, \\ y_{\mathrm{VP}} = k\sqrt{(y_{\mathrm{CCD}} - y_{\mathrm{CCD}o})^2 + (y_{\mathrm{CCD}} - y_{\mathrm{CCD}o})^2}\sin(\theta_{\mathrm{CCD}a} + \Delta\theta) + y_{\mathrm{CGH}o}. \end{cases} \tag{3}$$

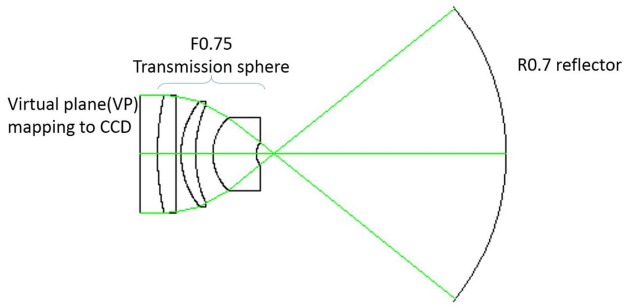

Fig. 4. Simulation of F0.75 transmission sphere.

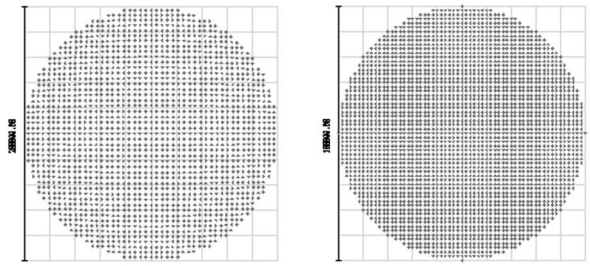

Fig. 5. Cosine distortion of F0.75 transmission sphere: (a) distorted points after transmission, and (b) uniform grid on mirror.

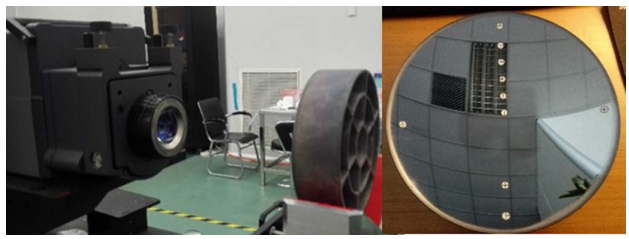

Fig. 6. Distortion calibration of the F0.75 transmission sphere.

3. EXPERIMENT

A. SFM with Large Distortion

The SFMs were Zernike surfaces with plane symmetric terms up to 41 to control the high-order off-axis aberrations due to the extremely large field of view (FOV). For its curvature change tempestuously, it needs high position pointing accuracy for deterministic fabrication.

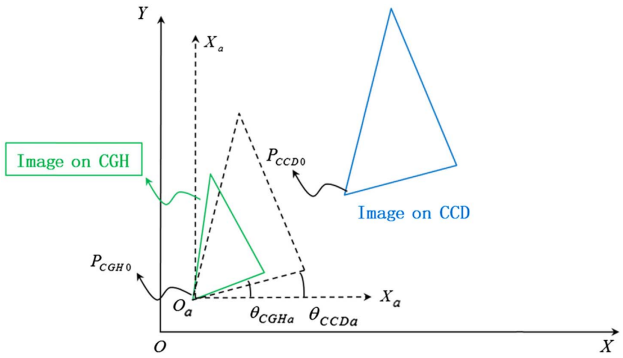

Fig. 7. Schematic diagram of the affine transformation relationship between CCD and CGH.

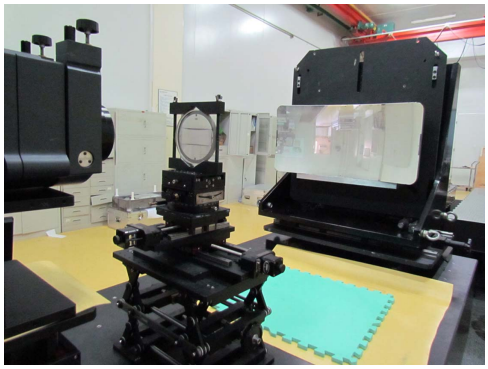

Fig. 8. Optical path in testing of the SFM.

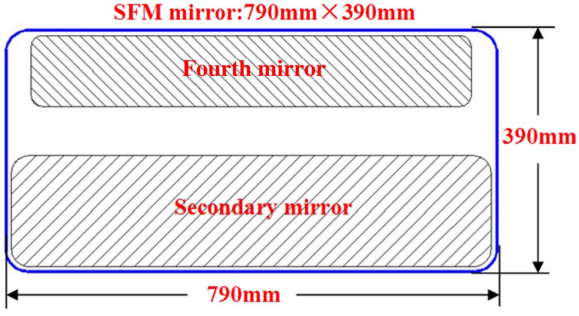

Fig. 9. Dimensions of the SFM mirror.

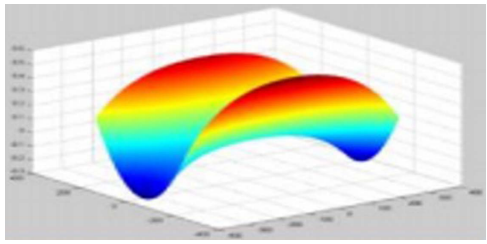

Fig. 10. Departure from best sphere fit of the SFM.

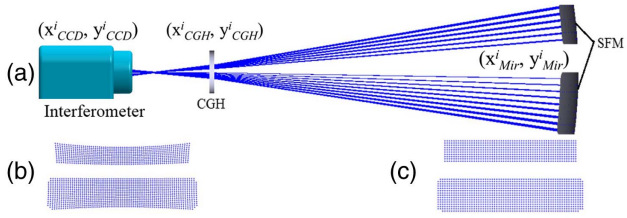

Fig. 11. Optical layout for testing SFM: (a) testing layout, (b) distorted spot diagram on CGH, and (c) uniform spot diagram on SFM.

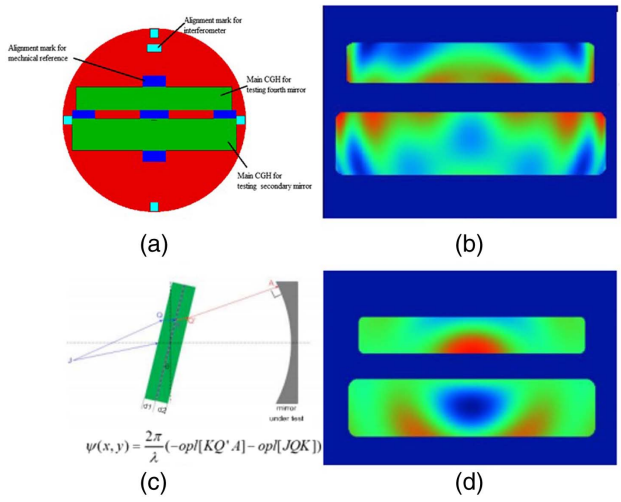

Fig. 12. CGH design based on ray tracing: (a) CGH function zones, (b) result of polynomial fitting, (c) sketch of ray tracing, and (d) result of ray tracing.

As shown in Figs. 8 and 9, the SFMs have long stripe shapes that are difficult for mechanical mounting. A tradeoff is to make the SFMs on a single 790 mm × 390 mm SiC substrate, then fabricate and test the two mirrors together. The departure from best sphere fit of the SFM shown in Fig. 10. This not only reduces mounting difficulty, but also eases the whole system alignment.

B. Testing Optical Path Design

The layout of optical testing is shown in Fig. 11, and the first-order design is finished. CGH was set 175.1 mm behind the focus spot. The phase distribution of CGH was calculated as shown in Fig. 11. As shown in Figs. 11(b) and 11(c), significant mapping distortion exists in the test data. The uniform spot diagram on SFM shown in Fig. 11(c) is traced to the distorted spot diagram on CGH shown in Fig. 11(b).

As shown in Figs. 11(b) and 11(c), due to the size limit of CGH, a serious mapping distortion exists. CGH design result shown in Fig. 12, and CGH picture is Fig. 13. The distortion coefficient is 0.6. Considering the cosine distortion of the transmission sphere, the total distortion coefficient is 0.612. The maximum position error for processing will reach 70 mm. The mapping distortion must be corrected.

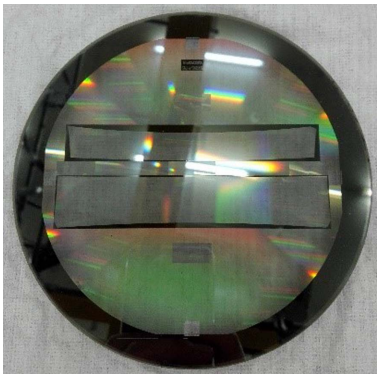

Fig. 13. CGH for the SFM.

C. Distortion Correction and Accuracy Check

The misalignment was checked by calculating the difference of mark image positions, which were measured by the profilometer. As shown in Table 1, E_x and E_y are the misalignments in the x and y directions, and $E_{\text{synthetist}}$ is the synthetical error; the maximum synthetical position error is 0.783 mm, which can satisfy the requirement of IBF.

Before final polishing, the surface error is 0.087λ RMS. The final polishing by IBF is shown in Fig. 14 and its result is shown in Fig. 15. Even though the IBF process can further improve the figure accuracy, 0.0433λ RMS already meets the specification defined by the prototype designer.

Table 1. Corrected Error of Marks

No.	1	2	3	4	5	6
E_x	0.388	0.209	0.503	−0.547	0.039	0.461
E_y	0.680	0.205	0.598	−0.198	0.199	−0.268
$E_{\text{synthetist}}$	0.783	0.292	0.781	0.582	0.204	0.534

(a) (b)

Fig. 14. Final polishing of SFM: (a) polishing in IBF, and (b) final mirror.

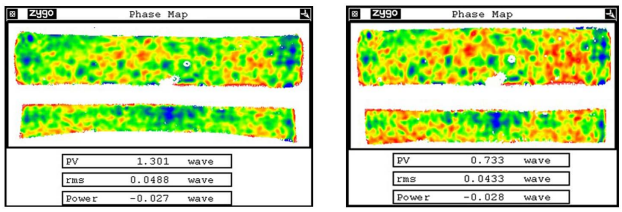

(a) (b)

Fig. 15. (a) Direct testing result, and (b) surface error distribution after distortion correction.

4. CONCLUSION

Freeform surfaces bring better performance in optical systems, but they are hard to test and fabricate. In this paper, a mapping distortion correction method was proposed in null testing of freeform surfaces. To improve the mapping distortion efficiency and generate improved precision, the freeform testing was separated into three parts and calibrated respectively to improve precision. The proposed distortion correction method is simple, rapid, and operable. Results show that the high-precision accuracy could satisfy deterministic fabrications, such as magnetorheological finishing (MRF) and IBF.

Funding. National Natural Science Foundation of China (NSFC) (61605202); Chinese Academy of Sciences Key Project (CAS Key Project) (QYZDJ-SSW-JSC038-02).

REFERENCES

1. I. Kaya, K. P. Thompson, and J. P. Rolland, "Edge clustered fitting grids for φ-polynomial characterization of freeform optical surfaces," Opt. Express **19**, 26962–26974 (2011).
2. T. Yang, G. F. Jin, and J. Zhu, "Automated design of freeform imaging systems," Light Sci. Appl. **6**, e17081 (2017).
3. M. Beier, D. Stumpf, U. D. Zeitner, A. Gebhardt, J. Hartung, S. Risse, R. Eberhardt, H. Gross, and A. Tünnermann, "Measuring position and figure deviation of freeform mirrors with computer generated holograms," in *Freeform Optics* (2015), paper FT3B.2.
4. X. Zhang and H. Hu, "Testing and alignment of freeform-based multimirror telescopes," Proc. SPIE **9578**, 95780B (2015).
5. D. Malacara, *Optical Shop Testing*, 3rd ed. (2006), pp. 483–484.
6. A. Ono and J. C. Wyant, "Aspherical mirror testing using a CGH with small errors," Appl. Opt. **24**, 560–563 (1985).
7. L. Fazhi, L. Xiao, Z. Jing-Li, X. Dong-Lin, Z. Li-Gong, and Z. Xue-Jun, "Test of off-axis aspheric surfaces with CGH," Opt. Precis. Eng. **4**, 709–716 (2011).
8. L. Rui-Gang, Z. Li-Gong, X. Dong-Lin, and Z. Xuejun, "Calibration method for projection distortion in interferometric testing high order and off-axis aspheric surface with big aperture," Opt. Precis. Eng. **14**, 533–538 (2006).
9. M. Novak, C. Zhao, and J. H. Burge, "Distortion mapping correction in aspheric null testing," Proc. SPIE **7063**, 706313 (2008).
10. M. Li, L. Xiao, and X. Donglin, "Design of CGH for testing large off-axis asphere by considering mapping distortion," Opt. Precis. Eng. **23**, 1246–1253 (2015).
11. Z. Zhang, R. Wang, T. Hao, C. Guo, D. Xue, and X. Zhang, "Fabrication of a high-accuracy phase-type computer-generated hologram by physical vapor deposition," Appl. Opt. **57**, F31–F36 (2018).
12. R. Parks, "Computer generated holograms as fixtures for testing optical elements," in *Optical Design and Fabrication (Freeform, IODC, OFT)*, OSA Technical Digest (Optical Society of America, 2017), paper JTh4B.4.
13. Y. Ogihara and Y. Sakamoto, "Fast calculation method of a CGH for a patch model using a point-based method," Appl. Opt. **54**, A76–A83 (2015).
14. C. Pruss, H. J. Tiziani, and S. Reichelt, "Absolute interferometric test of aspheres by use of twin computer-generated holograms," Appl. Opt. **42**, 4468–4479 (2003).
15. T. Kim, J. H. Burge, Y. Lee, and S. Kim, "Null test for a highly paraboloidal mirror," Appl. Opt. **43**, 3614–3618 (2004).
16. W. Wang, "The testing of aspheric surface with a combination method of CGH and null optical system," J. Appl. Opt. **06**, 50–53 (1991).
17. F. Y. Pan and J. Burge, "Efficient testing of segmented aspherical mirrors by use of reference plate and computer-generated holograms. I. Theory and system optimization," Appl. Opt. **43**, 5303–5312 (2004).
18. G. Pariani, C. Bertarelli, A. Bianco, F. Schaal, and C. Pruss, "Characterization of photochromic computer-generated holograms for optical testing," Proc. SPIE **8450**, 845010 (2012).
19. J. H. Burge, "Applications of computer-generated holograms for interferometric measurement of large aspheric optics," Proc. SPIE **2576**, 258–269 (1995).

20. M. J. Thomson and M. R. Taghizadeh, "Computer-generated holograms in interferometric testing," Opt. Eng. **43**, 2541–2548 (2004).
21. M. Hamdan, F. J. Moyano, and D. Schuhardt, "Demonstration of accuracy and flexibility of using CGH test plates for measuring aspheric surfaces," Proc. SPIE **3134**, 1195–1201 (1997).
22. C. F. Ho, Z. R. Yu, C. H. Kuo, and W. Y. Hsu, "Study on measurement of 160 mm convex hyperbolic mirror for cassegrain reflecting system," Proc. SPIE **8486**, 84860Q (2012).
23. Z. S. Gao, "Analysis of coincidence tolerance between F′ and C for the transmission spheres with small F-number," Chin. J. Lasers **31**, 186–189 (2004).